Theory of Sound Field Synthesis

Hagen Wierstorf

Assessment of IP-based Applications, Technische Universität Berlin

Jens Ahrens

Quality and Usability Lab, Technische Universität Berlin

Fiete Winter, Frank Schultz, Sascha Spors

Institue of Communications Engineering, Universität Rostock

Contents

1
Introduction

THIS DOCUMENT provides mathematical derivations of the equations that are implemented in the Sound Field Synthesis Toolbox.[1]

We decided to create the Toolbox and this documentation in order to fully allow for the principle of *reproducible research*[2] in the research area of sound field synthesis (SFS). Like other fields that involve signal processing, the study of SFS implies implementing a multitude of algorithms and running numerical simulations on a computer. As a consequence, the outcome of the algorithms are easily vulnerable to implementation errors which cannot completely be avoided.[3]

Functions derived in the theoretical chapter that are implemented in the toolbox are accompanied by a link to the corresponding function. All figures in this document have a link in the form of ☞ which is a link to a folder containing all the data and scripts in order to reproduce the single figures.

This document is mainly based on the PhD thesis of Hagen Wierstorf.[4] It starts with a small introduction to the history of spatial sound presentation and presents afterwards the theory of sound field synthesis, including the derivation of lots of different driving functions. All functions that come with a name tag like #D:wfs:pw are implemented in the Sound Field Synthesis Toolbox and referenced in the code using the tag. In Chap. **??** an index of all tags is presented with the corresponding page and equation number where it can be found in this document.

1.1 Spatial Sound Presentation

The first ever practical attempt of spatial sound reproduction dates back to 1881, only five years after the invention of the first monaural transducer. Back then, two parallel telephone channels were used to transmit recorded music to the homes of the listeners.[5] The basic idea was the ability to influence the interaural differences between the two ear signals of the listener. That was achieved by recording a sound scene with two microphones placed at different positions and feeding the recorded signals to the two telephone channels.

Later on the idea advanced to the technique of *binaural presentation* where the basic principle is to recreate the ear signals at both ears as they would appear in reality. This can be achieved by placing two microphones in the ears of the listener for recording and playing the recorded signals back via headphones afterwards. Binaural presentation has advanced in the last

[1] The Toolbox is available at https://github.com/sfstoolbox/sfs/ and was first described in H. Wierstorf and S. Spors. "Sound Field Synthesis Toolbox". In: *132nd Audio Engineering Society Convention*. 2012, eBrief 50

[2] For one of the pioneers see D. L. Donoho et al. "Reproducible Research in Computational Harmonic Analysis". *Computing in Science & Engineering* 11.1 (2009), pp. 8–18

[3] Compare D. C. Ince, L. Hatton, and J. Graham-Cumming. "The case for open computer programs". *Nature* 482.7386 (2012), pp. 485–88

[4] H. Wierstorf. "Perceptual Assessment of Sound Field Synthesis". PhD thesis. Technische Universität Berlin, 2014.

[5] T. du Moncel. "The international exhibition and congress of electricity at Paris". *Nature* October 20 (1881), pp. 585–89.
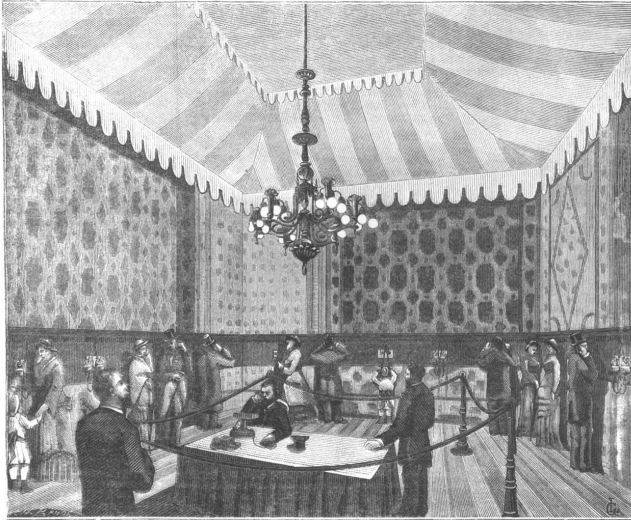
decades by measuring the acoustical transmission paths between a source and the ears of a listener, so called Head-Related Transfer Functions (HRTFs). Afterwards these can be used to create any sound scene as long as the required HRTFs are available.

Spatial sound presentation via loudspeakers started in the 1930s, the time when Blumlein invented the stereophonic recording and reproduction[6] and Steinberg and Snow discussed the idea of the acoustical curtain.[7] The original idea of the latter was to create a sound field that mimics the real sound scene. Their practical implementation with two or three loudspeakers was not able to achieve this. With such low numbers of loudspeakers the sound field is only controllable at single points in space. This corresponds to the classical stereophonic setup consisting of a fixed listener position between the two loudspeakers at a distance of around 2 m. The human head has a diameter of around 20 cm and hence only one ear can be placed at the point where the sound field is as desired. But as Steinberg and Snow discovered for their acoustic curtain, the spatial perception of the listener is not disturbed as long as she does not move too far away from a line on which every point has the same distance to both loudspeakers. By staying on that line the listener perceives an auditory event in the center of both loudspeakers, if the same acoustical signal is played through them. If the amplitude of one of the loudspeakers is changed the auditory event is moved between the two speakers. The connection of the amplitude difference between the loudspeakers and the actual position of the auditory event is empirical and is described by so called panning laws.[8] If the listener leaves the central line, the position of the auditory event will always be located at the position of one of the two loudspeakers. The area in which the spatial perception of the auditory scene works without considerable impairments is called the *sweet-spot* of a given loudspeaker setup. It is indicated by the blue color in Figure 1.2. To explain why the spatial perception of the listener is correct at the sweet-spot although the sound field is not, the theory of *summing localization* was introduced by Warncke in 1941.[9]

In the last years the stereophonic setup was expanded to 5.0 surround and even larger setups[10] and the panning laws were formulated in a more general

[6] A. D. Blumlein. "Improvements in and relating to Sound-transmission, Sound-recording and Sound-reproducing Systems". *Journal of the Audio Engineering Society* 6.2 (1958), pp. 91–98, 130

[7] J. Steinberg and W. B. Snow. "Symposium on wire transmission of symphonic music and its reproduction in auditory perspective: Physical Factors". *Bell System Technical Journal* 13.2 (1934), pp. 245–58.

[8] D. M. Leakey. "Some Measurements on the Effects of Interchannel Intensity and Time Differences in Two Channel Sound Systems". *The Journal of the Acoustical Society of America* 31.7 (1959), pp. 977–86

[9] A discussion is provided in J. Blauert. *Spatial Hearing*. The MIT Press, 1997, p. 204

[10] E.g. K. Hamasaki, K. Hiyama, and H. Okumura. "The 22.2 Multichannel Sound System and Its Application". In: *118th Audio Engineering Society Convention*. 2005, Paper 6406

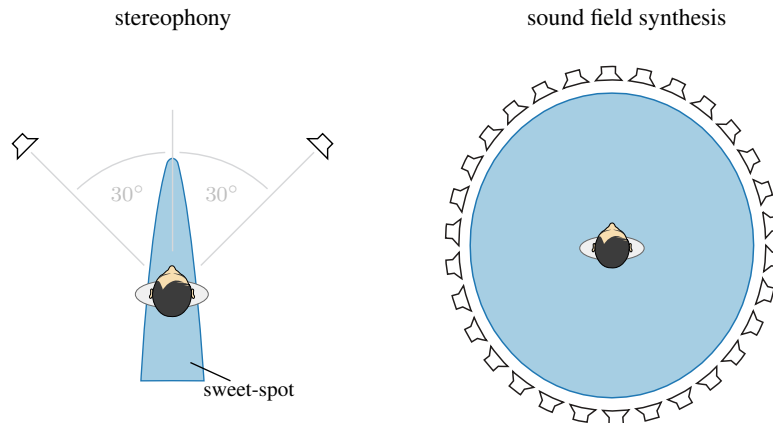stereophony   sound field synthesis

30°   30°

sweet-spot

Figure 1.2: Loudspeaker setups for two channel stereophony and sound field synthesis. The area marked in blue describes the positions were the listener can move to and still perceives the same spatial impression. This area is smaller for stereophonic setups and is called the sweet-spot. The figure of the stereophony setup is a modified version of J. Ahrens. *Analytic Methods of Sound Field Synthesis*. New York: Springer, 2012, Fig. 1.1. ☞

way dealing with setups using multiple loudspeakers.[11] These approaches could not fix the sweet-spot problem, but added a richer spatial impression because sound is no longer restricted to come from the front.

Before 5.0 surround there were other approaches to enhance the spatial impression of stereophony. From the 1970s onwards quadrophony and Ambisonics[12] were developed in order to provide a surround experience with four loudspeakers. The basic idea of Ambisonics is comparable to nowadays Near-Field Compensated Higher Order Ambisonics (NFC-HOA) for a larger number of loudspeakers: to describe an extended sound field by spherical basis functions that can be synthesized by any spherical or circular loudspeaker setup. In practice, the restriction of the limited number of loudspeakers has led to the usage of only two spherical basis functions. The results are loudspeaker signals that are comparable to the case of panning in stereophony with the difference of more active loudspeakers.[13] If more than four loudspeakers and more than two basis functions are applied the term is changed to Higher Order Ambisonics (HOA) to highlight this fact. For the perceptual side of Ambisonics the sweet-spot problem exists as well. The explanation of this sweet-spot is only partly covered by the theory of summing localization, because that theory is not well investigated for several sound sources coming from all directions. This provoked a high number of different optimizations of the loudspeaker signals by the Ambisonics community.

All of the methods described so far are able to provide a convincing spatial impression at a specific listener position within the loudspeaker setup. That means none of them can handle an equally good spatial impression for a bigger audience.

In the late 1980s the old idea of Steinberg and Snow to reproduce a complete sound field came to new life due to the fact that now arrangements of more than 100 loudspeakers became possible.[14] This high number of loudspeakers is needed: for controlling an extended sound field up to 20 kHz, loudspeaker spacings under 1 cm are required. Small distances like that are not possible in practice. Nonetheless, the experience has shown that even with larger distances reasonable sound field approximations are possible. Some of them provide equal spatial impression in the whole listening area, as indicated by the blue color in Figure 1.2. Methods trying to achieve this

[11] V. Pulkki. "Virtual Sound Source Positioning Using Vector Base Amplitude Panning". *Journal of the Audio Engineering Society* 45.6 (1997), pp. 456–66

[12] M. A. Gerzon. "Periphony: With-Height Sound Reproduction". *Journal of the Audio Engineering Society* 21.1 (1973), pp. 2–10.

[13] E.g. M. Frank. "Phantom Sources using Multiple Loudspeakers". PhD thesis. University of Music and Performing Arts Graz, 2013.

[14] A. Berkhout. "A holographic approach to acoustic control". *Journal of the Audio Engineering Society* 36.12 (1988), pp. 977–95.

goal are summarized under the term sound field synthesis (SFS). This document focusses on the two SFS techniques Wave Field Synthesis (WFS) and NFC-HOA that are explained in detail in the next chapter.
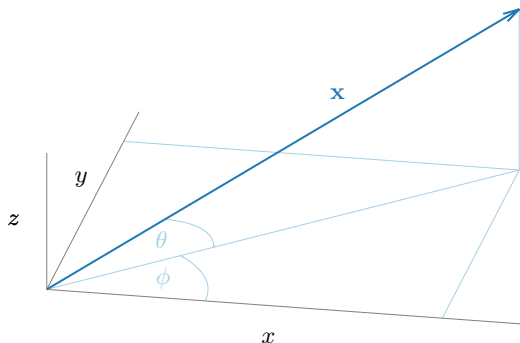
1.2 Mathematical Definitions

Figure 1.3: Coordinate system used in this thesis. The vector $\mathbf{x}$ can also be described by its length, its azimuth angle ϕ, and its elevation θ. ☞

Coordinate system Figure 1.3 shows the coordinate system that is used in the following chapters. A vector $\mathbf{x}$ can be described by its position (x, y, z) in space or by its length, azimuth angle $\phi \in [0, 2\pi[$, and elevation $\theta \in \left[-\frac{\pi}{2}, \frac{\pi}{2}\right]$. The azimuth is measured counterclockwise and elevation is positive for positive z-values.

Fourier transformation Let s be an absolute integrable function, t, ω real numbers, then the temporal Fourier transform is defined as[15]

$$S(\omega) = \mathcal{F}\{s(t)\} = \int_{-\infty}^{\infty} s(t)\mathrm{e}^{-\mathrm{i}\omega t} \ \mathrm{d}t \ .\tag{1}$$

In the same way the inverse temporal Fourier transform is defined as

$$s(t) = \mathcal{F}^{-1}\{S(\omega)\} = \frac{1}{2\pi}\int_{-\infty}^{\infty} S(\omega)\mathrm{e}^{\mathrm{i}\omega t} \ \mathrm{d}\omega \ .\tag{2}$$

[15] R. N. Bracewell. *The Fourier Transform and its Applications*. Boston: McGraw Hill, 2000.
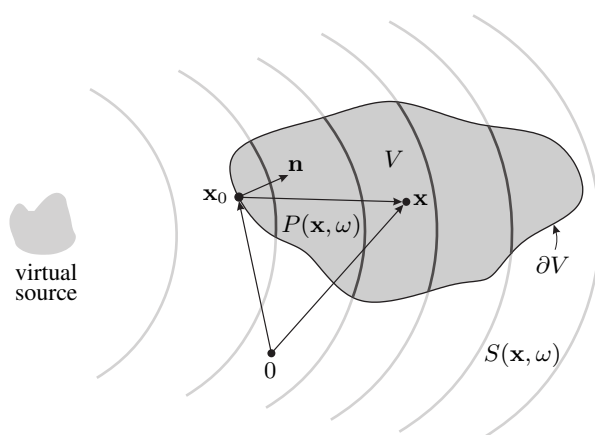
2
Theory of Sound Field Synthesis

THE PROBLEM of sound field synthesis can be formulated as follows.[1] Assume a volume $V \subset \mathbb{R}^n$ which is free of any sources and sinks, surrounded by a distribution of monopole sources on its surface ∂V. The pressure $P(\mathbf{x}, \omega)$ at a point $\mathbf{x} \in V$ is then given by the *single-layer potential*

$$P(\mathbf{x}, \omega) = \oint_{\partial V} D(\mathbf{x}_0, \omega) G(\mathbf{x} - \mathbf{x}_0, \omega) \ \mathrm{d}A(\mathbf{x}_0) \, , \qquad (3)$$

#single:layer

where $G(\mathbf{x} - \mathbf{x}_0, \omega)$ denotes the sound propagation of the source at location $\mathbf{x}_0 \in \partial V$, and $D(\mathbf{x}_0, \omega)$ its weight, usually referred to as *driving function*. The sources on the surface are called *secondary sources* in sound field synthesis, analogue to the case of acoustical scattering problems. The single-layer potential can be derived from the Kirchhoff-Helmholtz integral.[2] The challenge in sound field synthesis is to solve the integral with respect to $D(\mathbf{x}_0, \omega)$ for a desired sound field $P = S$ in V. It has unique solutions which Zotter and Spors[3] explicitly showed for the spherical case and Fazi[4] for the planar case.

In the following the single-layer potential for different dimensions is discussed. An approach to formulate the desired sound field S is described and finally it is shown how to derive the driving function D.

[1] Small parts of this section are published in H. Wierstorf, A. Raake, and S. Spors. "Binaural assessment of multi-channel reproduction". In: *The technology of binaural listening*. Ed. by J. Blauert. New York: Springer, 2013, pp. 255–78.

[2] E. G. Williams. *Fourier Acoustics*. San Diego: Academic Press, 1999.

[3] F. Zotter and S. Spors. "Is sound field control determined at all frequencies? How is it related to numerical acoustics?" In: *52nd Audio Engineering Society Conference*. 2013, Paper 1.3

[4] F. M. Fazi. "Sound Field Reproduction". PhD thesis. University of Southampton, 2010, Chap. 4.3.

2.1 Solution for Special Geometries: Near-Field Compensated Higher Order Ambisonics and Spectral Division Method

The integral equation (3) states a Fredholm equation of first kind with a Green's function as kernel. This type of equation can be solved in a straightforward manner for geometries that have a complete set of orthogonal basis functions. Then the involved functions are expanded into the basis functions ψ_n as[5]

$$G(\mathbf{x} - \mathbf{x}_0, \omega) = \sum_{n=1}^{N} \tilde{G}_n(\omega)\, \psi_n^*(\mathbf{x}_0)\psi_n(\mathbf{x}) \tag{4}$$

$$D(\mathbf{x}_0, \omega) = \sum_{n=1}^{N} \tilde{D}_n(\omega)\, \psi_n(\mathbf{x}_0) \tag{5}$$

$$S(\mathbf{x}, \omega) = \sum_{n=1}^{N} \tilde{S}_n(\omega)\, \psi_n(\mathbf{x}) \;, \tag{6}$$

where $\tilde{G}_n, \tilde{D}_n, \tilde{S}_n$ denote the series expansion coefficients and $\langle \psi_n, \psi_{n'} \rangle = 0$ for $n \neq n'$. Introducing these three equations into (3) one gets

$$\tilde{D}_n(\omega) = \frac{\tilde{S}_n(\omega)}{\tilde{G}_n(\omega)} \;. \tag{7}$$

This means that the Fredholm equation (3) states a convolution. For geometries where the required orthogonal basis functions exist, (7) follows directly via the convolution theorem.[6] Due to the division of the desired sound field by the spectrum of the Green's function this kind of approach has been named Spectral Division Method (SDM).[7] For circular and spherical geometries the term Near-Field Compensated Higher Order Ambisonics (NFC-HOA) is more common due to the corresponding basis functions. "Near-field compensated" highlights the usage of point sources as secondary sources in contrast to Ambisonics and Higher Order Ambisonics (HOA) that assume plane waves as secondary sources.

The challenge is to find a set of basis functions for a given geometry. In the following paragraphs three simple geometries and their widely known sets of basis functions will be discussed.

2.1.1 Spherical Geometries

The spherical harmonic functions constitute a basis for a spherical secondary source distribution in $\mathbb{R}^3$ and can be defined as[8]

$$Y_n^m(\theta, \phi) = (-1)^m \sqrt{\frac{(2n+1)(n-|m|)!}{4\pi(n+|m|)!}}\, P_n^{|m|}(\sin\theta)\mathrm{e}^{im\phi} \;, \tag{8}$$

$$n = 0, 1, 2, \ldots \qquad m = -n, \ldots, n$$

where $P_n^{|m|}$ are the associated Legendre functions. Note that this function may also be defined in a slightly different way, omitting the $(-1)^m$ factor, see for example Williams.[9]

[5] Compare P. M. Morse and H. Feshbach. *Methods of Theoretical Physics*. Minneapolis: Feshbach Publishing, 1981, p. 940.

[6] Compare G. B. Arfken and H. J. Weber. *Mathematical Methods for Physicists*. Amsterdam: Elsevier, 2005, p. 1013.

[7] J. Ahrens and S. Spors. "Sound Field Reproduction Using Planar and Linear Arrays of Loudspeakers". *IEEE Transactions on Audio, Speech, and Language Processing* 18.8 (2010), pp. 2038–50

sphharmonics.m
asslegendre.m

[8] N. A. Gumerov and R. Duraiswami. *Fast Multipole Methods for the Helmholtz Equation in Three Dimensions*. Amsterdam: Elsevier, 2004, (12.153), $\sin\theta$ is used here instead of $\cos\theta$ due to the use of another coordinate system, compare Figure 2.1 from Gumerov and Duraiswami and Figure 1.3 in this thesis.

[9] Williams, op. cit., (6.20).

The complex conjugate of Y_n^m is given by negating the degree m as

$$Y_n^m(\theta, \phi)^* = Y_n^{-m}(\theta, \phi) \ . \tag{9}$$

For a spherical secondary source distribution with a radius of R_0 the sound field can be calculated by a convolution along the surface. The driving function is then given by a simple division as[10]

$$D_{\text{spherical}}(\theta_0, \phi_0, \omega) =$$
$$\frac{1}{R_0^2} \sum_{n=0}^{\infty} \sum_{m=-n}^{n} \sqrt{\frac{2n+1}{4\pi}} \frac{\breve{S}_n^m(\theta_s, \phi_s, r_s, \omega)}{\breve{G}_n^0(\frac{\pi}{2}, 0, \omega)} Y_n^m(\theta_0, \phi_0) \ , \tag{10}$$

where $\breve{S}_n^m$ denote the spherical expansion coefficients of the source model, θ_s and ϕ_s its directional dependency, and $\breve{G}_n^0$ the spherical expansion coefficients of a secondary point source that is located at the north pole of the sphere with $\mathbf{x}_0 = (0, 0, R_0)$ and is given as[11]

$$\breve{G}_n^0(\tfrac{\pi}{2}, 0, \omega) = -\mathrm{i}\frac{\omega}{c} \sqrt{\frac{2n+1}{4\pi}}\, h_n^{(2)}\left(\frac{\omega}{c} R_0\right) \ , \tag{11}$$

where $h_n^{(2)}$ describes the spherical Hankel function of n-th order and second kind.

2.1.2 Circular Geometries

The following functions build a basis in $\mathbb{R}^2$ for a circular secondary source distribution[12]

$$\Phi_m(\phi) = \mathrm{e}^{\mathrm{i}m\phi} \ . \tag{12}$$

The complex conjugate of Φ_m is given by negating the degree m as

$$\Phi_m(\phi)^* = \Phi_{-m}(\phi) \ . \tag{13}$$

For a circular secondary source distribution with a radius of R_0 the driving function can be calculated by a convolution along the surface of the circle as explicitly shown by Ahrens[13] and is then given as

$$D_{\text{circular}}(\phi_0, \omega) = \frac{1}{2\pi R_0} \sum_{m=-\infty}^{\infty} \frac{\breve{S}_m(\phi_s, r_s, \omega)}{\breve{G}_m(0, \omega)} \Phi_m(\phi_0) \ , \tag{14}$$

where $\breve{S}_m$ denotes the circular expansion coefficients for the source model, ϕ_s its directional dependency, and $\breve{G}_m$ the circular expansion coefficients for a secondary line source with

$$\breve{G}_m(0, \omega) = -\frac{\mathrm{i}}{4} H_m^{(2)}\left(\frac{\omega}{c} R_0\right) \ , \tag{15}$$

where $H_m^{(2)}$ describes the Hankel function of m-th order and second kind.

2.1.3 Planar Geometries

The basis functions for a planar secondary source distribution located on the xz-plane in $\mathbb{R}^3$ are given as

$$\Lambda(k_x, k_z, x, z) = \mathrm{e}^{-\mathrm{i}(k_x x + k_z z)} \ , \tag{16}$$

[10] J. Ahrens. *Analytic Methods of Sound Field Synthesis*. New York: Springer, 2012, (3.21). The $\frac{1}{2\pi}$ term is wrong in (3.21) and omitted here, compare the `errata` and F. Schultz and S. Spors. "Comparing Approaches to the Spherical and Planar Single Layer Potentials for Interior Sound Field Synthesis". *Acta Acustica* 100.5 (2014), pp. 900–11, (24).

[11] F. Schultz and S. Spors. "Comparing Approaches to the Spherical and Planar Single Layer Potentials for Interior Sound Field Synthesis". *Acta Acustica* 100.5 (2014), pp. 900–11, (25).

[12] Williams, op. cit.

[13] J. Ahrens and S. Spors. "On the Secondary Source Type Mismatch in Wave Field Synthesis Employing Circular Distributions of Loudspeakers". In: *127th Audio Engineering Society Convention*. 2009, Paper 7952.

where k_x, k_z are entries in the wave vector $\mathbf{k}$ with $k^2 = (\frac{\omega}{c})^2$. The complex conjugate is given by negating k_x and k_z as

$$\Lambda(k_x, k_z, x, z)^* = \Lambda(-k_x, -k_z, x, z) \ . \tag{17}$$

For an infinitely long secondary source distribution located on the xz-plane the driving function can be calculated by a two-dimensional convolution along the plane as[14]

$$D_{\text{planar}}(x_0, \omega) = \frac{1}{4\pi^2} \iint_{-\infty}^{\infty} \frac{\breve{S}(k_x, y_s, k_z, \omega)}{\breve{G}(k_x, 0, k_z, \omega)} \Lambda(k_x, x_0, k_z, z_0) \ \mathrm{d}k_x \ \mathrm{d}k_z \ , \tag{18}$$

where $\breve{S}$ denotes the planar expansion coefficients for the source model, y_s its positional dependency, and $\breve{G}$ the planar expansion coefficients of a secondary point source with[15]

$$\breve{G}(k_x, 0, k_z, \omega) = -\frac{\mathrm{i}}{2} \frac{1}{\sqrt{(\frac{\omega}{c})^2 - k_x^2 - k_z^2}} \ , \tag{19}$$

for $(\frac{\omega}{c})^2 > (k_x^2 + k_z^2)$.

For the planar and the following linear geometries the Fredholm equation is solved for a non compact space V, which leads to an infinite and non-denumerable number of basis functions as opposed to the denumerable case for compact spaces.[16]

2.1.4   Linear Geometries

The basis functions for a linear secondary source distribution located on the x-axis are given as

$$\chi(k_x, x) = \mathrm{e}^{-\mathrm{i}k_x x} \ . \tag{20}$$

The complex conjugate is given by negating k_x as

$$\chi(k_x, x)^* = \chi(-k_x, x) \ . \tag{21}$$

For an infinitely long secondary source distribution located on the x-axis the driving function for $\mathbb{R}^2$ can be calculated by a convolution along this axis as[17]

$$D_{\text{linear}}(x_0, \omega) = \frac{1}{2\pi} \int_{-\infty}^{\infty} \frac{\breve{S}(k_x, y_s, \omega)}{\breve{G}(k_x, 0, \omega)} \chi(k_x, x_0) \ \mathrm{d}k_x \ , \tag{22}$$

where $\breve{S}$ denotes the linear expansion coefficients for the source model, y_s, z_s its positional dependency, and $\breve{G}$ the linear expansion coefficients of a secondary line source with

$$\breve{G}(k_x, 0, \omega) = -\frac{\mathrm{i}}{2} \frac{1}{\sqrt{(\frac{\omega}{c})^2 - k_x^2}} \ , \tag{23}$$

for $0 < |k_x| < |\frac{\omega}{c}|$.

2.2   High Frequency Approximation: Wave Field Synthesis

The single-layer potential (3) satisfies the homogeneous Helmholtz equation both in the interior and exterior regions V and $V^* := \mathbb{R}^n \setminus (V \cup \partial V)$. If

[14] J. Ahrens. *Analytic Methods of Sound Field Synthesis*. New York: Springer, 2012, (3.65).

[15] Schultz and Spors, op. cit., (65).

[16] Ibid.

[17] Compare (3.73) in Ahrens, op. cit.

$D(\mathbf{x}_0, \omega)$ is continuous, the pressure $P(\mathbf{x}, \omega)$ is continuous when approaching the surface ∂V from the inside and outside. Due to the presence of the secondary sources at the surface ∂V, the gradient of $P(\mathbf{x}, \omega)$ is discontinuous when approaching the surface. The strength of the secondary sources is then given by the differences of the gradients approaching ∂V from both sides as[18]

$$D(\mathbf{x}_0, \omega) = \partial_{\mathbf{n}} P(\mathbf{x}_0, \omega) + \partial_{-\mathbf{n}} P(\mathbf{x}_0, \omega) \,, \qquad (24)$$
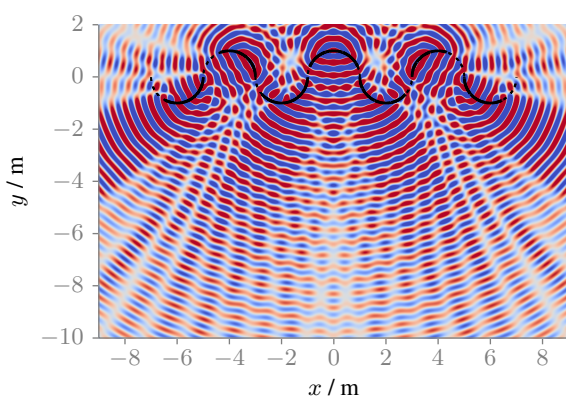
where $\partial_{\mathbf{n}} := \langle \nabla, \mathbf{n} \rangle$ is the directional gradient in direction $\mathbf{n}$ – see Figure 2.1. Due to the symmetry of the problem the solution for an infinite planar boundary ∂V is given as

$$D(\mathbf{x}_0, \omega) = -2\partial_{\mathbf{n}} S(\mathbf{x}_0, \omega) \,, \qquad (25)$$

where the pressure in the outside region is the mirrored interior pressure given by the source model $S(\mathbf{x}, \omega)$ for $\mathbf{x} \in V$. The integral equation resulting from introducing (25) into (3) for a planar boundary ∂V is known as *Rayleigh's first integral equation*. This solution is identical to the explicit solution for planar geometries (18) in $\mathbb{R}^3$ and for linear geometries (22) in $\mathbb{R}^2$.

A solution of (24) for arbitrary boundaries can be found by applying the *Kirchhoff* or *physical optics approximation*.[19] In acoustics this is also known as *determining the visible elements* for the high frequency boundary element method.[20] Here, it is assumed that a bent surface can be approximated by a set of small planar surfaces for which (25) holds locally. In general, this will be the case if the wave length is much smaller than the size of a planar surface patch and the position of the listener is far away from the secondary sources.[21] Additionally, only one part of the surface is active: the area that is illuminated from the incident field of the source model.

With this approximation also non-convex secondary source distributions can be used with WFS – compare Figure 2.2.[22] This was neglected in most of the literature so far, which postulates convex secondary source distributions.[23]

[18] Compare F. M. Fazi and P. A. Nelson. "Sound field reproduction as an equivalent acoustical scattering problem". *The Journal of the Acoustical Society of America* 134.5 (2013), pp. 3721–9

[19] See D. Colton and R. Kress. *Integral Equation Methods in Scattering Theory*. New York: Wiley, 1983, p.53–54

[20] E.g. D. W. Herrin et al. "A New Look at the High Frequency Boundary Element and Rayleigh Integral Approximations". In: *Noise & Vibration Conference and Exhibition*. 2003

[21] Compare the two assumptions in S. Spors and F. Zotter. "Spatial Sound Synthesis with Loudspeakers". In: *Cutting Edge in Spatial Audio, EAA Winter School*. 2013, pp. 32–37, made before (15), which lead to the derivation of the same window function in a more explicit way.

[22] See the appendix in M. Lax and H. Feshbach. "On the Radiation Problem at High Frequencies". *The Journal of the Acoustical Society of America* 19.4 (1947), pp. 682–90

[23] E.g. S. Spors, R. Rabenstein, and J. Ahrens. "The Theory of Wave Field Synthesis Revisited". In: *124th Audio Engineering Society Convention*. 2008, Paper 7358

Figure 2.2: Sound pressure of a point source synthesized with WFS (68). The secondary source distribution is shown in black, whereby inactive sources are marked with a dashed line. Parameters: $\mathbf{x}_s = (0, 2.5, 0)\,\mathrm{m}$, $\mathbf{x}_{\mathrm{ref}} = (0, -3, 0)\,\mathrm{m}$, $f = 700\,\mathrm{Hz}$. ☞

The outlined approximation can be formulated by introducing a window function $w(\mathbf{x}_0)$ for the selection of the active secondary sources into (25) as

$$P(\mathbf{x}, \omega) \approx \oint_{\partial V} G(\mathbf{x}|\mathbf{x}_0, \omega) \underbrace{-2w(\mathbf{x}_0)\partial_{\mathbf{n}} S(\mathbf{x}_0, \omega)}_{D(\mathbf{x}_0, \omega)} \, \mathrm{d}A(\mathbf{x}_0) \,. \qquad (26)$$

One of the advantages of the applied approximation is that due to its local character the solution of the driving function (25) does not depend on the

geometry of the secondary sources. This dependency applies to the direct solutions presented in Section 2.1.

2.3 Sound Field Dimensionality

The single-layer potential (3) is valid for all $V \subset \mathbb{R}^n$. Consequentially, for practical applications a two-dimensional (2D) as well as a three-dimensional (3D) synthesis is possible. Two-dimensional is not referring to a synthesis in a plane only, but describes a setup that is independent of one dimension. For example, an infinite cylinder is independent of the dimension along its axis. The same is true for secondary source distributions in 2D synthesis. They exhibit line source characteristics and are aligned in parallel to the independent dimension. Typical arrangements of such secondary sources are a circular or a linear setup.

The characteristics of the secondary sources limit the set of possible sources which can be synthesized. For example, when using a 2D secondary source setup it is not possible to synthesize the amplitude decay of a point source.

For a 3D synthesis the involved secondary sources depend on all dimensions and exhibit point source characteristics. In this scenario classical secondary sources setups would be a sphere or a plane.
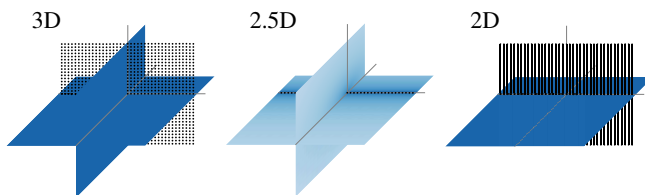
2.3.1 2.5D Synthesis

Figure 2.3: Sound pressure in decibel for secondary source distributions with different dimensionality all driven by the same signals. The sound pressure is color coded, lighter color corresponds to lower pressure. In the 3D case a planar distribution of point sources is applied, in the 2.5D case a linear distribution of point sources, and in the 2D case a linear distribution of line sources. ☞

In practice, the most common setups of secondary sources are 2D setups, employing cabinet loudspeakers. A cabinet loudspeaker does not show the characteristics of a line source, but of a point source. This dimensionality mismatch prevents perfect synthesis within the desired plane. The combination of a 2D secondary source setup with secondary sources that exhibit 3D characteristics has led to naming such configurations *2.5D synthesis*.[24] Such scenarios are associated with a wrong amplitude decay due to the inherent mismatch of secondary sources as is highlighted in Figure 2.3. In general, the amplitude is only correct at a given reference point $\mathbf{x}_{\text{ref}}$.

For a circular secondary source distribution with point source characteristic the 2.5D driving function can be derived by introducing expansion coefficients for the spherical case into the driving function (14). The equation is than solved for $\theta = 0°$ and $r_{\text{ref}} = 0$. This results in a 2.5D driving function given in Ahrens[25] as

$$D_{\text{circular,2.5D}}(\phi_0, \omega) = \frac{1}{2\pi R_0} \sum_{m=-\infty}^{\infty} \frac{\breve{S}_{|m|}^m(\frac{\pi}{2}, \phi_{\text{s}}, r_{\text{s}}, \omega)}{\breve{G}_{|m|}^m(\frac{\pi}{2}, 0, \omega)} \Phi_m(\phi_0) . \quad (27)$$

For a linear secondary source distribution with point source characteristics the 2.5D driving function is derived by introducing the linear expansion

[24] E. W. Start. "Direct Sound Enhancement by Wave Field Synthesis". PhD thesis. Technische Universiteit Delft, 1997

[25] Ibid., (3.49).

coefficients for a monopole source (40) into the driving function (22) and solving the equation for $y = y_{\text{ref}}$ and $z = 0$. This results in a 2.5D driving function given as[26]

$$D_{\text{linear},2.5\text{D}}(x_0, \omega) = \frac{1}{2\pi} \int_{-\infty}^{\infty} \frac{\breve{S}(k_x, y_{\text{ref}}, 0, \omega)}{\breve{G}(k_x, y_{\text{ref}}, 0, \omega)} \chi(k_x, x_0) \, dk_x \ . \quad (28)$$

A driving function for the 2.5D situation in the context of WFS and arbitrary 2D geometries of the secondary source distribution can be achieved by applying the far-field approximation[27] $H_0^{(2)}(\zeta) \approx \sqrt{\frac{2i}{\pi\zeta}} e^{-i\zeta}$ for $\zeta \gg 1$ to the 2D Green's function. Using this the following relationship between the 2D and 3D Green's functions can be established.

$$\underbrace{-\frac{i}{4} H_0^{(2)}\left(\frac{\omega}{c}|\mathbf{x} - \mathbf{x}_0|\right)}_{G_{2\text{D}}(\mathbf{x}-\mathbf{x}_0, \omega)} \approx \sqrt{2\pi \frac{c}{i\omega}|\mathbf{x} - \mathbf{x}_0|} \ \underbrace{\frac{1}{4\pi} \frac{e^{-i\frac{\omega}{c}|\mathbf{x}-\mathbf{x}_0|}}{|\mathbf{x} - \mathbf{x}_0|}}_{G_{3\text{D}}(\mathbf{x}-\mathbf{x}_0, \omega)} \ , \quad (29)$$

where $H_0^{(2)}$ denotes the Hankel function of second kind and zeroth order. Inserting this approximation into the single-layer potential for the 2D case results in

$$P(\mathbf{x}, \omega) = \oint_S \sqrt{2\pi \frac{c}{i\omega}|\mathbf{x} - \mathbf{x}_0|} \ D(\mathbf{x}_0, \omega) G_{3\text{D}}(\mathbf{x} - x0, \omega) \, dA(\mathbf{x}_0) \ . \quad (30)$$

If the amplitude correction is further restricted to one reference point $\mathbf{x}_{\text{ref}}$, the 2.5D driving function for WFS can be formulated as

$$D_{2.5\text{D}}(\mathbf{x}_0, \omega) = \underbrace{\sqrt{2\pi|\mathbf{x}_{\text{ref}} - \mathbf{x}_0|}}_{g_0} \sqrt{\frac{c}{i\omega}} \ D(\mathbf{x}_0, \omega) \ , \quad (31)$$

where g_0 is independent of $\mathbf{x}$.

2.4 Model-Based Rendering

Knowing the pressure field of the desired source $S(\mathbf{x}, \omega)$ is required in order to derive the driving signal for the secondary source distribution. It can either be measured, i.e. recorded, or modeled. While the former is known as *data-based rendering*, the latter is known as *model-based rendering*. For data-based rendering, the problem of how to capture a complete sound field still has to be solved. Avni et al. discuss some influences of the recording limitations on the perception of the reproduced sound field.[28] This thesis focusses on the perception of the synthesis part. Therefore it will consider only model-based rendering.

Frequently applied models in model-based rendering are plane waves, point sources, or sources with a prescribed complex directivity. In the following the models used within the Sound Field Synthesis Toolbox are presented.

Plane Wave The source model for a plane wave is given as[29]

$$S(\mathbf{x}, \omega) = A(\omega)\mathrm{e}^{-\mathrm{i}\frac{\omega}{c}\mathbf{n}_k\mathbf{x}} , \tag{32}$$

#S:pw

where $A(\omega)$ denotes the frequency spectrum of the source and $\mathbf{n}_k$ a unit vector pointing into the direction of the plane wave.

Transformed in the temporal domain this becomes

$$s(\mathbf{x}, t) = a(t) * \delta\left(t - \frac{\mathbf{n}_k\mathbf{x}}{c}\right) , \tag{33}$$

#s:pw

where $a(t)$ is the Fourier transformation of the frequency spectrum $A(\omega)$.

The expansion coefficients for spherical basis functions are given as[30]

$$\breve{S}_n^m(\theta_k, \phi_k, \omega) = 4\pi\mathrm{i}^{-n}Y_n^{-m}(\theta_k, \phi_k) , \tag{34}$$

where (ϕ_k, θ_k) is the radiating direction of the plane wave.

In a similar manner the expansion coefficients for circular basis functions are given as

$$\breve{S}_m(\phi_\mathrm{s}, \omega) = \mathrm{i}^{-n}\Phi_{-m}(\phi_\mathrm{s}) . \tag{35}$$

The expansion coefficients for linear basis functions are given as after Ahrens[31]

$$\breve{S}(k_x, y, \omega) = 2\pi\,\delta(k_x - k_{x,\mathrm{s}})\,\chi(k_{y,\mathrm{s}}, y) , \tag{36}$$

where $(k_{x,\mathrm{s}}, k_{y,\mathrm{s}})$ points into the radiating direction of the plane wave.

Point Source The source model for a point source is given by the three dimensional Green's function as[32]

$$S(\mathbf{x}, \omega) = A(\omega)\frac{1}{4\pi}\frac{\mathrm{e}^{-\mathrm{i}\frac{\omega}{c}|\mathbf{x}-\mathbf{x}_\mathrm{s}|}}{|\mathbf{x}-\mathbf{x}_\mathrm{s}|} , \tag{37}$$

#S:ps

where $\mathbf{x}_\mathrm{s}$ describes the position of the point source.

Transformed to the temporal domain this becomes

$$s(\mathbf{x}, t) = a(t) * \frac{1}{4\pi}\frac{1}{|\mathbf{x}-\mathbf{x}_\mathrm{s}|}\delta\left(t - \frac{|\mathbf{x}-\mathbf{x}_\mathrm{s}|}{c}\right) . \tag{38}$$

#s:ps

```
greens_function_mono.m
greens_function_imp.m
```

[28] A. Avni et al. "Spatial perception of sound fields recorded by spherical microphone arrays with varying spatial resolution". *The Journal of the Acoustical Society of America* 133.5 (2013), pp. 2711–21.

[29] E. G. Williams. *Fourier Acoustics*. San Diego: Academic Press, 1999, p. 21, (2.24). Williams defines the Fourier transform with transposed signs as $F(\omega) = \int f(t)\mathrm{e}^{\mathrm{i}\omega t}$. This leads also to changed signs in his definitions of the Green's functions and field expansions.
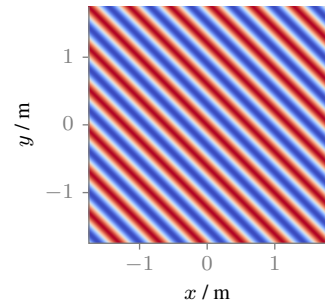

Figure 2.4: Sound pressure for a monochromatic plane wave (32) going into the direction $(1, 1, 0)$. Parameters: $f = 800\,\mathrm{Hz}$. ☞

[30] Ahrens, op. cit., (2.38)

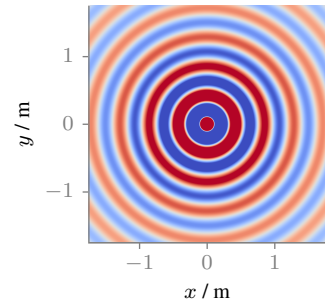[31] ibid., (C.5)

[32] Williams, op. cit., (6.73)

Figure 2.5: Sound pressure for a monochromatic point source (37) placed at $(0, 0, 0)$. Parameters: $f = 800\,\mathrm{Hz}$. ☞

The expansion coefficients for spherical basis functions are given as[33]

$$\breve{S}_n^m(\theta_s, \phi_s, r_s, \omega) = -\mathrm{i}\frac{\omega}{c}\, h_n^{(2)}\!\left(\frac{\omega}{c}r_s\right) Y_n^{-m}(\theta_s, \phi_s)\;, \qquad (39)$$

where (ϕ_s, θ_s, r_s) describes the position of the point source.

The expansion coefficients for linear basis functions are given as[34]

$$\breve{S}(k_x, y, \omega) = -\frac{\mathrm{i}}{4}\, H_0^{(2)}\!\left(\sqrt{(\tfrac{\omega}{c})^2 - k_x^2}\,|y - y_s|\right) \chi(-k_x, x_s)\;, \qquad (40)$$

for $|k_x| < |\frac{\omega}{c}|$ and with (x_s, y_s) describing the position of the point source.

3D Dipole Source The source model for a three dimensional dipole source is given by the directional derivative of the three dimensional Green's function with respect to $\mathbf{n}_s$ defining the orientation of the dipole source.

$$S(\mathbf{x}, \omega) = A(\omega)\left\langle \nabla_{\mathbf{x}_s}\!\left(\frac{1}{4\pi}\frac{\mathrm{e}^{-\mathrm{i}\frac{\omega}{c}|\mathbf{x}-\mathbf{x}_s|}}{|\mathbf{x}-\mathbf{x}_s|}\right), \mathbf{n}_s\right\rangle$$
$$= A(\omega)\frac{1}{4\pi}\left(\frac{1}{|\mathbf{x}-\mathbf{x}_s|} + \mathrm{i}\frac{\omega}{c}\right)\frac{\langle\mathbf{x}-\mathbf{x}_s, \mathbf{n}_s\rangle}{|\mathbf{x}-\mathbf{x}_s|^2}\mathrm{e}^{-\mathrm{i}\frac{\omega}{c}|\mathbf{x}-\mathbf{x}_s|}\;. \quad \text{\#S:dps} \tag{41}$$

Transformed to the temporal domain this becomes

$$s(\mathbf{x}, t) = a(t)*\left(\frac{1}{|\mathbf{x}-\mathbf{x}_s|} + \mathcal{F}^{-1}\left\{\frac{\mathrm{i}\omega}{c}\right\}\right)*\frac{\langle\mathbf{x}-\mathbf{x}_s, \mathbf{n}_s\rangle}{4\pi|\mathbf{x}-\mathbf{x}_s|^2}\delta\!\left(t - \frac{|\mathbf{x}-\mathbf{x}_s|}{c}\right)\;. \tag{42}$$

#s:dps

Line Source The source model for a line source is given by the two dimensional Green's function as[35]

$$S(\mathbf{x}, \omega) = -A(\omega)\frac{\mathrm{i}}{4}\, H_0^{(2)}\!\left(\frac{\omega}{c}|\mathbf{x}-\mathbf{x}_s|\right)\;. \tag{43}$$

#S:ls

Applying the large argument approximation of the Hankel function[36] and transformed to the temporal domain this becomes

$$s(\mathbf{x}, t) = a(t)*\mathcal{F}^{-1}\left\{\sqrt{\frac{c}{\mathrm{i}\omega}}\right\}*\sqrt{\frac{1}{8\pi}}\frac{1}{\sqrt{|\mathbf{x}-\mathbf{x}_s|}}\delta\!\left(t - \frac{|\mathbf{x}-\mathbf{x}_s|}{c}\right)\;. \tag{44}$$

#s:ls

The expansion coefficients for circular basis functions are given as

$$\breve{S}_m(\phi_s, r_s, \omega) = -\frac{\mathrm{i}}{4}\, H_m^{(2)}\!\left(\frac{\omega}{c}r_s\right)\Phi_{-m}(\phi_s)\;. \tag{45}$$

The expansion coefficients for linear basis functions are given as

$$\breve{S}(k_x, y_s, \omega) = -\frac{\mathrm{i}}{2}\frac{1}{\sqrt{(\tfrac{\omega}{c})^2 - k_x^2}}\chi(k_y, y_s)\;. \tag{46}$$

2.5 Driving Functions

In the following, driving functions for Near-Field Compensated Higher Order Ambisonics, the Spectral Division Method and Wave Field Synthesis are derived for spherical, circular, and linear secondary source distributions. Among the possible combinations of methods and secondary sources not all
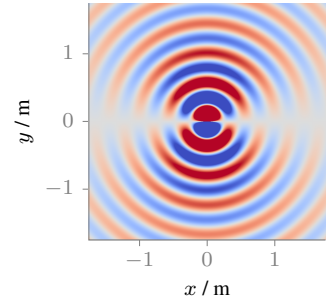
[33] Ahrens, op. cit., (2.37).

[34] Ibid., (C.10).

Figure 2.6: Sound pressure for a monochromatic 3D dipole source (41) placed at $(0, 0, 0)$. Parameters: $f = 800\,\text{Hz}$. ☞
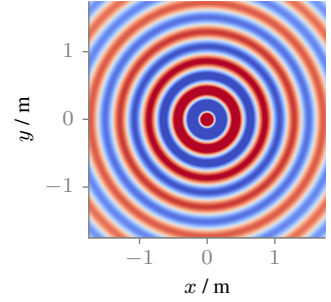
[35] ibid., (8.47)
[36] ibid., (4.23)

Figure 2.7: Sound pressure for a monochromatic line source (43) placed at $(0, 0, 0)$. Parameters: $f = 800\,\text{Hz}$. ☞

are meaningful. Hence, only the relevant ones will be presented. The same holds for the introduced source models of plane waves, point sources, line sources and focused sources. Ahrens and Spors[37] in addition have considered Spectral Division Method driving functions for planar secondary source distributions.

The driving functions are given in the temporal-frequency domain. For some of them, especially in the case of WFS an analytic solution in the temporal domain exists and is presented. For NFC-HOA, temporal-domain implementations for the 2.5D cases are available for a plane wave and a point source as source models. The derivation of the implementation is not explicitly shown here, but is described in Spors et al.[38]

The 2.5D cases are illustrated in the following by companion figures, because only those cases will be investigated in the remainder of this thesis.

2.5.1 Near-Field Compensated Higher Order Ambisonics and Spectral Division Method

Plane Wave   For a spherical secondary source distribution with radius R_0 the spherical expansion coefficients of a plane wave (34) and of the Green's function for a point source (11) are inserted into (10) and yield[39]

$$D_{\text{spherical}}(\theta_0, \phi_0, \omega) = -A(\omega) \frac{4\pi}{R_0^2} \sum_{n=0}^{\infty} \sum_{m=-n}^{n} \frac{\mathrm{i}^{-n} Y_n^{-m}(\theta_k, \phi_k)}{\mathrm{i}\frac{\omega}{c} h_n^{(2)}\left(\frac{\omega}{c}R_0\right)} Y_n^m(\theta_0, \phi_0) \ .$$

(47)

#D:hoa:pw:3D

For a circular secondary source distribution with radius R_0 the circular expansion coefficients of a plane wave (35) and of the Green's function for a line source (15) are inserted into (14) and yield[40]

$$D_{\text{circular}}(\phi_0, \omega) = -A(\omega) \frac{2\mathrm{i}}{\pi R_0} \sum_{m=-\infty}^{\infty} \frac{\mathrm{i}^{-m} \Phi_{-m}(\phi_k)}{H_m^{(2)}(\frac{\omega}{c}R_0)} \Phi_m(\phi_0) \ .$$

(48)

#D:hoa:pw:2D

For a circular secondary source distribution with radius R_0 and point source as Green's function the 2.5D driving function is given by inserting the spherical expansion coefficients for a plane wave (34) and a point source (39) into (27) as

$$D_{\text{circular, 2.5D}}(\phi_0, \omega) = -A(\omega) \frac{2}{R_0} \sum_{m=-\infty}^{\infty} \frac{\mathrm{i}^{-|m|} \Phi_{-m}(\phi_k)}{\mathrm{i}\frac{\omega}{c} h_{|m|}^{(2)}\left(\frac{\omega}{c}R_0\right)} \Phi_m(\phi_0) \ .$$

(49)

#D:hoa:pw:2.5D

For an infinite linear secondary source distribution located on the x-axis the 2.5D driving function is given by inserting the linear expansion coefficients for a point source as Green's function (23) and a plane wave (36) into (28) and exploiting the fact that $(\frac{\omega}{c})^2 - k_{x_\mathrm{s}}$ is constant. Assuming $0 \leq |k_{x_\mathrm{s}}| \leq |\frac{\omega}{c}|$ this results in[41]

$$D_{\text{linear, 2.5D}}(x_0, \omega) = A(\omega) \frac{4\mathrm{i}\chi(k_y, y_{\text{ref}})}{H_0^{(2)}(k_y y_{\text{ref}})} \chi(k_x, x_0) \ .$$

(50)

#D:sdm:pw:2.5D

Transfered to the temporal domain this results in[42]

[37] Ahrens and Spors, op. cit.

[38] S. Spors, V. Kuscher, and J. Ahrens. "Efficient realization of model-based rendering for 2.5-dimensional near-field compensated higher order Ambisonics". In: *IEEE Workshop on Applications of Signal Processing to Audio and Acoustics*. 2011, pp. 61–64

[39] Schultz and Spors, op. cit., (96).

`driving_function_mono_nfchoa_pw.m`
`driving_function_mono_sdm_pw.m`
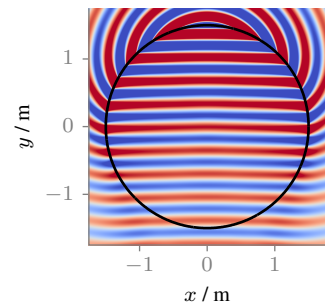`driving_function_imp_nfchoa_pw.m`

Figure 2.8: Sound pressure of a monochromatic plane wave synthesized with 2.5D NFC-HOA (49). Parameters: $\mathbf{n}_k = (0, -1, 0)$, $\mathbf{x}_{\text{ref}} = (0, 0, 0)$, $f = 1\,\text{kHz}$. ☞

[40] Compare J. Ahrens and S. Spors. "On the Secondary Source Type Mismatch in Wave Field Synthesis Employing Circular Distributions of Loudspeakers". In: *127th Audio Engineering Society Convention*. 2009, Paper 7952, (16)

[41] J. Ahrens and S. Spors. "Sound Field Reproduction Using Planar and Linear Arrays of Loudspeakers". *IEEE Transactions on Audio, Speech, and Language Processing* 18.8 (2010), pp. 2038–50, (17)

[42] ibid., (18)

$$d_{\text{linear, 2.5D}}(x_0, t) = h(t) * a\left(t - \frac{x_0}{c}\sin\phi_k - \frac{y_{\text{ref}}}{c}\sin\phi_k\right), \qquad (51)$$

where ϕ_k denotes the azimuth direction of the plane wave and

$$h(t) = \mathcal{F}^{-1}\left\{ \frac{4\mathrm{i}}{H_0^{(2)}(k_y y_{\text{ref}})} \right\}. \qquad (52)$$

The advantage of this result is that it can be implemented by a simple weighting and delaying of the signal, plus one convolution with $h(t)$. The same holds for the driving functions of WFS as presented in the next section.

Point Source For a spherical secondary source distribution with radius R_0 the spherical coefficients of a point source (39) and of the Green's function (11) are inserted into (10) and yield

$$D_{\text{spherical}}(\theta_0, \phi_0, \omega) =$$
$$A(\omega)\frac{1}{R_0^2}\sum_{n=0}^{\infty}\sum_{m=-n}^{n}\frac{h_n^{(2)}(\frac{\omega}{c}r_{\text{s}})Y_n^{-m}(\theta_{\text{s}},\phi_{\text{s}})}{h_n^{(2)}(\frac{\omega}{c}R_0)}Y_n^m(\theta_0,\phi_0). \qquad (53)$$

#D:hoa:ps:3D

For a circular secondary source distribution with radius R_0 and point source as secondary sources the 2.5D driving function is given by inserting the spherical coefficients (39) and (11) into (27) as

$$D_{\text{circular, 2.5D}}(\phi_0, \omega) = A(\omega)\frac{1}{2\pi R_0}\sum_{m=-\infty}^{\infty}\frac{h_{|m|}^{(2)}(\frac{\omega}{c}r_s)\Phi_{-m}(\phi_{\text{s}})}{h_{|m|}^{(2)}(\frac{\omega}{c}R_0)}\Phi_m(\phi_0). \qquad (54)$$

#D:hoa:ps:2.5D

For an infinite linear secondary source distribution located on the x-axis and point sources as secondary sources the 2.5D driving function for a point source is given by inserting the corresponding linear expansion coefficients (40) and (23) into (28). Assuming $0 \leq |k_x| < |\frac{\omega}{c}|$ this results in[43]

$$D_{\text{linear, 2.5D}}(x_0, \omega) =$$
$$A(\omega)\int_{-\infty}^{\infty}\frac{H_0^{(2)}\left(\sqrt{(\frac{\omega}{c})^2 - k_x^2}\,(y_{\text{ref}} - y_{\text{s}})\right)\chi(-k_x, x_{\text{s}})}{H_0^{(2)}\left(\sqrt{(\frac{\omega}{c})^2 - k_x^2}\,y_{\text{ref}}\right)}\chi(k_x, x_0)\,\mathrm{d}k_x. \qquad (55)$$

#D:sdm:ps:2.5D

Line Source For a circular secondary source distribution with radius R_0 and line sources as secondary sources the driving function is given by inserting the circular coefficients (45) and (15) into (14) as

$$D_{\text{circular}}(\phi_0, \omega) = A(\omega)\frac{1}{2\pi R_0}\sum_{m=-\infty}^{\infty}\frac{H_m^{(2)}(\frac{\omega}{c}r_s)\Phi_{-m}(\phi_{\text{s}})}{H_m^{(2)}(\frac{\omega}{c}R_0)}\Phi_m(\phi_0). \quad (56)$$

For an infinite linear secondary source distribution located on the x-axis and line sources as secondary sources the driving function is given by inserting the linear coefficients (46) and (15) into (22) as

$$D_{\text{linear}}(x_0, \omega) = A(\omega)\frac{1}{2\pi}\int_{-\infty}^{\infty}\chi(k_y, y_s)\chi(k_x, x_0)\,\mathrm{d}k_x. \qquad (57)$$

driving_function_mono_nfchoa_ps.m
driving_function_imp_nfchoa_ps.m

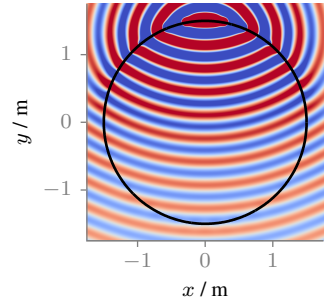Figure 2.9: Sound pressure for a monochromatic point source synthesized by 2.5D NFC-HOA (54). Parameters: $\mathbf{x}_{\text{s}} = (0, 2.5, 0)\,\mathrm{m}$, $\mathbf{x}_{\text{ref}} = (0, 0, 0)$, $f = 1\,\mathrm{kHz}$. ☞

[43] Compare (4.53) in Ahrens, op. cit.

Focused Source Focused sources mimic point or line sources that are located inside the audience area. For the single-layer potential the assumption is that the audience area is free from sources and sinks. However, a focused source is neither of them. It represents a sound field that converges towards a focal point and diverges afterwards. This can be achieved by reversing the driving function of a point or line source in time which is known as time reversal focusing.[44]

Nonetheless, the single-layer potential should not be solved for focused sources without any approximation. In the near field of a source, evanescent waves[45] appear for spatial frequencies $k_x > |\frac{\omega}{c}|$. They decay exponentially with the distance from the source. An exact solution for a focused source is supposed to include these evanescent waves around the focal point. That is only possible by applying very large amplitudes to the secondary sources.[46] Since the evanescent waves decay rapidly and are hence not influencing the perception, they can easily be omitted. For corresponding driving functions for focused sources without the evanescent part of the sound field see Spors and Ahrens[47] for SDM and Ahrens and Spors[48] for NFC-HOA.

In this thesis only focused sources in WFS will be considered.

2.5.2 Wave Field Synthesis

In the following, the driving functions for WFS in the frequency and temporal domain for selected source models are presented. The temporal domain functions consist of a filtering of the source signal and a weighting and delaying of the individual secondary source signals. This property allows for a very efficient implementation of WFS driving functions in the temporal domain. It is one of the main advantages of WFS in comparison to most of the NFC-HOA/SDM solutions discussed above.

Plane Wave By inserting the source model of a plane wave (32) into (25) and (31) it follows

$$D(\mathbf{x}_0, \omega) = 2w(\mathbf{x}_0)A(\omega)\mathrm{i}\frac{\omega}{c}\mathbf{n}_k\mathbf{n}_{\mathbf{x}_0}\mathrm{e}^{-\mathrm{i}\frac{\omega}{c}\mathbf{n}_k\mathbf{x}_0} \;, \tag{58}$$

#D:wfs:pw

$$D_{2.5\mathrm{D}}(\mathbf{x}_0, \omega) = 2g_0 w(\mathbf{x}_0)A(\omega)\sqrt{\mathrm{i}\frac{\omega}{c}}\mathbf{n}_k\mathbf{n}_{\mathbf{x}_0}\mathrm{e}^{-\mathrm{i}\frac{\omega}{c}\mathbf{n}_k\mathbf{x}_0} \;. \tag{59}$$

#D:wfs:pw:2.5D

Transfered to the temporal domain via an inverse Fourier transform (2), it follows

$$d(\mathbf{x}_0, t) = 2a(t) * h(t) * w(\mathbf{x}_0)\mathbf{n}_k\mathbf{n}_{\mathbf{x}_0} \delta\Big(t - \frac{\mathbf{n}_k\mathbf{x}_0}{c}\Big) \;, \tag{60}$$

#d:wfs:pw

$$d_{2.5\mathrm{D}}(\mathbf{x}_0, t) = 2g_0 a(t) * h_{2.5\mathrm{D}}(t) * w(\mathbf{x}_0)\mathbf{n}_k\mathbf{n}_{\mathbf{x}_0} \delta\Big(t - \frac{\mathbf{n}_k\mathbf{x}_0}{c}\Big) \;, \tag{61}$$

#d:wfs:pw:2.5D

where

$$h(t) = \mathcal{F}^{-1}\Big\{\mathrm{i}\frac{\omega}{c}\Big\} \;, \tag{62}$$

#wfs:preeq

[44] S. Yon, M. Tanter, and M. Fink. "Sound focusing in rooms: The time-reversal approach". *The Journal of the Acoustical Society of America* 113.3 (2003), pp. 1533–43

[45] Williams, op. cit., p. 24

[46] Compare Fig. 2a in S. Spors and J. Ahrens. "Reproduction of Focused Sources by the Spectral Division Method". In: *International Symposium on Communications, Control and Signal Processing*. 2010

[47] ibid.

[48] J. Ahrens and S. Spors. "Spatial encoding and decoding of focused virtual sound sources". In: *International Symposium on Ambisonics and Spherical Acoustics*. 2009

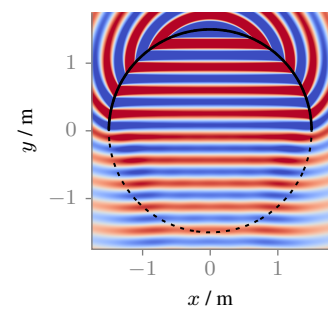`driving_function_mono_wfs_pw.m`
`driving_function_imp_wfs_pw.m`

Figure 2.10: Sound pressure for a monochromatic plane wave synthesized by 2.5D WFS (59). Parameters: $\mathbf{n}_k = (0, -1, 0)$, $\mathbf{x}_{\mathrm{ref}} = (0, 0, 0)$, $f = 1\,\mathrm{kHz}$. ☞

and

$$h_{2.5\text{D}}(t) = \mathcal{F}^{-1}\left\{\sqrt{\mathrm{i}\frac{\omega}{c}}\right\} \tag{63}$$

denote the so called pre-equalization filters in WFS.

The window function $w(\mathbf{x}_0)$ for a plane wave as source model can be calculated after Spors et al. as[49]

$$w(\mathbf{x}_0) = \begin{cases} 1 & \mathbf{n}_k\mathbf{n}_{\mathbf{x}_0} > 0 \\ 0 & \text{else} \end{cases} \tag{64}$$

[49] S. Spors, R. Rabenstein, and J. Ahrens. "The Theory of Wave Field Synthesis Revisited". In: *124th Audio Engineering Society Convention*. 2008, Paper 7358.

Point Source By inserting the source model for a point source (37) into (25) and (31) it follows

$$D(\mathbf{x}_0, \omega) =$$
$$\frac{1}{2\pi}A(\omega)w(\mathbf{x}_0)\left(\mathrm{i}\frac{\omega}{c} + \frac{1}{|\mathbf{x}_0 - \mathbf{x}_\mathrm{s}|}\right)\frac{(\mathbf{x}_0 - \mathbf{x}_\mathrm{s})\mathbf{n}_{\mathbf{x}_0}}{|\mathbf{x}_0 - \mathbf{x}_\mathrm{s}|^2}\mathrm{e}^{-\mathrm{i}\frac{\omega}{c}|\mathbf{x}_0 - \mathbf{x}_\mathrm{s}|} \,, \tag{65}$$
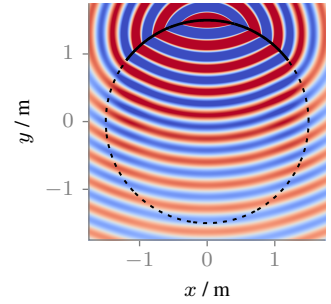
Figure 2.11: Sound pressure for a monochromatic point source synthesized by 2.5D WFS (68). Parameters: $\mathbf{x}_\mathrm{s} = (0, 2.5, 0)\,\mathrm{m}$, $\mathbf{x}_\mathrm{ref} = (0, 0, 0)$, $f = 1\,\mathrm{kHz}$. ☞

$$D_{2.5\text{D}}(\mathbf{x}_0, \omega) =$$
$$\frac{g_0}{2\pi}A(\omega)w(\mathbf{x}_0)\sqrt{\mathrm{i}\frac{\omega}{c}}\left(1 + \frac{1}{\mathrm{i}\frac{\omega}{c}|\mathbf{x}_0 - \mathbf{x}_\mathrm{s}|}\right)\frac{(\mathbf{x}_0 - \mathbf{x}_\mathrm{s})\mathbf{n}_{\mathbf{x}_0}}{|\mathbf{x}_0 - \mathbf{x}_\mathrm{s}|^2}\mathrm{e}^{-\mathrm{i}\frac{\omega}{c}|\mathbf{x}_0 - \mathbf{x}_\mathrm{s}|} \,. \tag{66}$$

Under the assumption of $|\mathbf{x}_0 - \mathbf{x}_\mathrm{s}| \gg 1$ (65) and (66) can be approximated by

$$D(\mathbf{x}_0, \omega) = \frac{1}{2\pi}A(\omega)w(\mathbf{x}_0)\mathrm{i}\frac{\omega}{c}\frac{(\mathbf{x}_0 - \mathbf{x}_\mathrm{s})\mathbf{n}_{\mathbf{x}_0}}{|\mathbf{x}_0 - \mathbf{x}_\mathrm{s}|^{3/2}}\mathrm{e}^{-\mathrm{i}\frac{\omega}{c}|\mathbf{x}_0 - \mathbf{x}_\mathrm{s}|} \,, \tag{67}$$

$$D_{2.5\text{D}}(\mathbf{x}_0, \omega) =$$
$$\frac{g_0}{2\pi}A(\omega)w(\mathbf{x}_0)\sqrt{\mathrm{i}\frac{\omega}{c}}\frac{(\mathbf{x}_0 - \mathbf{x}_\mathrm{s})\mathbf{n}_{\mathbf{x}_0}}{|\mathbf{x}_0 - \mathbf{x}_\mathrm{s}|^{3/2}}\mathrm{e}^{-\mathrm{i}\frac{\omega}{c}|\mathbf{x}_0 - \mathbf{x}_\mathrm{s}|} \,, \tag{68}$$

which is the traditional formulation of a point source in WFS as given for the 2.5D case in Verheijen.[50] It has the advantage that its temporal domain version could again be implemented as a simple weighting- and delaying-mechanism. This is the default driving function for a point source in the Sound Field Synthesis Toolbox.

[50] E. Verheijen. "Sound Reproduction by Wave Field Synthesis". PhD thesis. Technische Universiteit Delft, 1997, (2.22a), whereby r corresponds to $|\mathbf{x}_0 - \mathbf{x}_\mathrm{s}|$ and $\cos\varphi$ to $\frac{(\mathbf{x}_0 - \mathbf{x}_\mathrm{s})\mathbf{n}_{\mathbf{x}_0}}{|\mathbf{x}_0 - \mathbf{x}_\mathrm{s}|}$.

Transferred to the temporal domain via an inverse Fourier transform (2) it follows

$$d(\mathbf{x}_0, t) = \frac{1}{2\pi}a(t) * h(t) * w(\mathbf{x}_0)\frac{(\mathbf{x}_0 - \mathbf{x}_\mathrm{s})\mathbf{n}_{\mathbf{x}_0}}{|\mathbf{x}_0 - \mathbf{x}_\mathrm{s}|^{3/2}}\delta\left(t - \frac{|\mathbf{x}_0 - \mathbf{x}_\mathrm{s}|}{c}\right) \,, \tag{69}$$

$$d_{2.5D}(\mathbf{x}_0, t) =$$

$$\frac{g_0}{2\pi} a(t) * h_{2.5D}(t) * w(\mathbf{x}_0) \frac{(\mathbf{x}_0 - \mathbf{x}_s)\mathbf{n}_{\mathbf{x}_0}}{|\mathbf{x}_0 - \mathbf{x}_s|^{3/2}} \delta\left(t - \frac{|\mathbf{x}_0 - \mathbf{x}_s|}{c}\right) .$$

$$(70)$$

#d:wfs:ps:2.5D

The window function $w(\mathbf{x}_0)$ for a point source as source model can be calculated after Spors at al. as[51]

$$w(\mathbf{x}_0) = \begin{cases} 1 & (\mathbf{x}_0 - \mathbf{x}_s)\mathbf{n}_{\mathbf{x}_0} > 0 \\ 0 & \text{else} \end{cases} \tag{71}$$

#wfs:ps:selection

Line Source By inserting the source model for a line source (43) into (25) and (31) and calculating the derivate of the Hankel function[52] it follows

$$D(\mathbf{x}_0, \omega) = -\frac{1}{2} A(\omega) w(\mathbf{x}_0) i \frac{\omega}{c} \frac{(\mathbf{x}_0 - \mathbf{x}_s)\mathbf{n}_{\mathbf{x}_0}}{|\mathbf{x}_0 - \mathbf{x}_s|} H_1^{(2)}\left(\frac{\omega}{c}|\mathbf{x}_0 - \mathbf{x}_s|\right) ,$$

$$(72)$$

#D:wfs:ls

$$D_{2.5D}(\mathbf{x}_0, \omega) =$$

$$-\frac{1}{2} g_0 A(\omega) w(\mathbf{x}_0) \sqrt{i \frac{\omega}{c}} \frac{(\mathbf{x}_0 - \mathbf{x}_s)\mathbf{n}_{\mathbf{x}_0}}{|\mathbf{x}_0 - \mathbf{x}_s|} H_1^{(2)}\left(\frac{\omega}{c}|\mathbf{x}_0 - \mathbf{x}_s|\right) .$$

$$(73)$$

#D:wfs:ls:2.5D

Applying $H_1^{(2)}(\zeta) \approx -\sqrt{\frac{2}{\pi i \zeta}} e^{-i\zeta}$ for $z \gg 1$ after Williams[53] and transfered to the temporal domain via an inverse Fourier transform (2) it follows

$$d(\mathbf{x}_0, t) = \sqrt{\frac{1}{2\pi}} a(t) * h(t) * w(\mathbf{x}0) \frac{(\mathbf{x}_0 - \mathbf{x}_s)\mathbf{n}_{\mathbf{x}_0}}{|\mathbf{x}_0 - \mathbf{x}_s|^{3/2}} \delta\left(t - \frac{|\mathbf{x}_0 - \mathbf{x}_s|}{c}\right) ,$$

$$(74)$$

#d:wfs:ls

$$d_{2.5D}(\mathbf{x}_0, t) =$$

$$g_0 \sqrt{\frac{1}{2\pi}} a(t) * \mathcal{F}^{-1}\left\{\sqrt{\frac{c}{i\omega}}\right\} * w(\mathbf{x}0) \frac{(\mathbf{x}_0 - \mathbf{x}_s)\mathbf{n}_{\mathbf{x}_0}}{|\mathbf{x}_0 - \mathbf{x}_s|^{3/2}} \delta\left(t - \frac{|\mathbf{x}_0 - \mathbf{x}_s|}{c}\right) .$$

$$(75)$$

The window function $w(\mathbf{x}_0)$ for a line source as source model can be calculated after Spors et al. as[54]

$$w(\mathbf{x}_0) = \begin{cases} 1 & (\mathbf{x}_0 - \mathbf{x}_s)\mathbf{n}_{\mathbf{x}_0} > 0 \\ 0 & \text{else} \end{cases} \tag{76}$$

#wfs:ls:selection

Focused Source As mentioned before, focused sources exhibit a field that converges in a focal point inside the audience area. After passing the focal point, the field becomes a diverging one as can be seen in Figure 2.13. In order to choose the active secondary sources, especially for circular or spherical geometries, the focused source also needs a direction $\mathbf{n}_s$.

secondary_source_selection.m

[51] Spors, Rabenstein, and Ahrens, op. cit.

driving_function_mono_wfs_ls.m
driving_function_imp_wfs_ls.m

[52] M. Abramowitz and I. A. Stegun. *Handbook of Mathematical Functions*. Washington: National Bureau of Standards, 1972, (9.1.30).
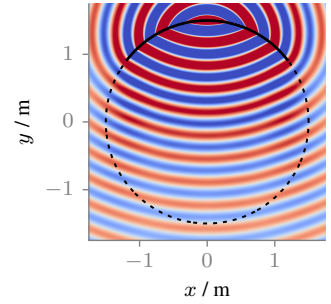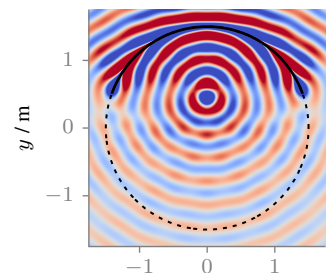
[53] Williams, op. cit., (4.23)

Figure 2.12: Sound pressure for a monochromatic line source synthesized by 2.5D WFS (73). Parameters: $\mathbf{x}_s = (0, 2.5, 0)\,\text{m}$, $\mathbf{x}_{\text{ref}} = (0, 0, 0)$, $f = 1\,\text{kHz}$. ☞

secondary_source_selection.m

[54] Spors, Rabenstein, and Ahrens, op. cit.

driving_function_mono_wfs_fs.m
driving_function_imp_wfs_fs.m

The driving function for a focused source are given by the time-reversed versions of the driving functions for a point source as

$$
\begin{aligned}
D(\mathbf{x}_0,\omega) = \\
\frac{1}{2\pi}A(\omega)w(\mathbf{x}_0)\left(\mathrm{i}\frac{\omega}{c}+\frac{1}{|\mathbf{x}_0-\mathbf{x}_\mathrm{s}|}\right)\frac{(\mathbf{x}_0-\mathbf{x}_\mathrm{s})\mathbf{n}_{\mathbf{x}_0}}{|\mathbf{x}_0-\mathbf{x}_\mathrm{s}|^2}\mathrm{e}^{\mathrm{i}\frac{\omega}{c}|\mathbf{x}_0-\mathbf{x}_\mathrm{s}|} \;,
\end{aligned}
$$

(77)

#D:wfs:fs:woapprox

$$
\begin{aligned}
D_{2.5\mathrm{D}}(\mathbf{x}_0,\omega) = \\
\frac{g_0}{2\pi}A(\omega)w(\mathbf{x}_0)\sqrt{\mathrm{i}\frac{\omega}{c}}\left(1+\frac{1}{\mathrm{i}\frac{\omega}{c}|\mathbf{x}_0-\mathbf{x}_\mathrm{s}|}\right)\frac{(\mathbf{x}_0-\mathbf{x}_\mathrm{s})\mathbf{n}_{\mathbf{x}_0}}{|\mathbf{x}_0-\mathbf{x}_\mathrm{s}|^2}\mathrm{e}^{\mathrm{i}\frac{\omega}{c}|\mathbf{x}_0-\mathbf{x}_\mathrm{s}|} \;,
\end{aligned}
$$

(78)

#D:wfs:fs:woapprox:2.5D

or by using an approximated point source as

$$
D(\mathbf{x}_0,\omega) = \frac{1}{2\pi}A(\omega)w(\mathbf{x}_0)\mathrm{i}\frac{\omega}{c}\frac{(\mathbf{x}_0-\mathbf{x}_\mathrm{s})\mathbf{n}_{\mathbf{x}_0}}{|\mathbf{x}_0-\mathbf{x}_\mathrm{s}|^{3/2}}\mathrm{e}^{\mathrm{i}\frac{\omega}{c}|\mathbf{x}_0-\mathbf{x}_\mathrm{s}|} \;,
$$

(79)

#D:wfs:fs

$$
D_{2.5\mathrm{D}}(\mathbf{x}_0,\omega) = \frac{g_0}{2\pi}A(\omega)w(\mathbf{x}_0)\sqrt{\mathrm{i}\frac{\omega}{c}}\frac{(\mathbf{x}_0-\mathbf{x}_\mathrm{s})\mathbf{n}_{\mathbf{x}_0}}{|\mathbf{x}_0-\mathbf{x}_\mathrm{s}|^{3/2}}\mathrm{e}^{\mathrm{i}\frac{\omega}{c}|\mathbf{x}_0-\mathbf{x}_\mathrm{s}|} \;.
$$

(80)

#D:wfs:fs:2.5D

As before for other source types, the approximated versions are the default driving functions for a focused source used in this thesis.

Transfered to the temporal domain via an inverse Fourier transform (2) it follows

$$
d(\mathbf{x}_0,t) = \frac{1}{2\pi}a(t)*h(t)*w(\mathbf{x}_0)\frac{(\mathbf{x}_0-\mathbf{x}_\mathrm{s})\mathbf{n}_{\mathbf{x}_0}}{|\mathbf{x}_0-\mathbf{x}_\mathrm{s}|^{3/2}}\delta\left(t+\frac{|\mathbf{x}_0-\mathbf{x}_\mathrm{s}|}{c}\right) \;,
$$

(81)

#d:wfs:fs

$$
\begin{aligned}
d_{2.5\mathrm{D}}(\mathbf{x}_0,t) = \\
\frac{g_0}{2\pi}a(t)*h_{2.5\mathrm{D}}(t)*w(\mathbf{x}_0)\frac{(\mathbf{x}_0-\mathbf{x}_\mathrm{s})\mathbf{n}_{\mathbf{x}_0}}{|\mathbf{x}_0-\mathbf{x}_\mathrm{s}|^{3/2}}\delta\left(t+\frac{|\mathbf{x}_0-\mathbf{x}_\mathrm{s}|}{c}\right) \;.
\end{aligned}
$$

(82)

#d:wfs:fs:2.5D

In this thesis a focused source always refers to the time-reversed version of a point source, but a focused line source can be defined in the same way starting from (72)

$$
D(\mathbf{x}_0,\omega) = -\frac{1}{2}A(\omega)w(\mathbf{x}_0)\mathrm{i}\frac{\omega}{c}\frac{(\mathbf{x}_0-\mathbf{x}_\mathrm{s})\mathbf{n}_{\mathbf{x}_0}}{|\mathbf{x}_0-\mathbf{x}_\mathrm{s}|}H_1^{(1)}\left(\frac{\omega}{c}|\mathbf{x}_0-\mathbf{x}_\mathrm{s}|\right) \;.
$$

(83)

#D:wfs:fs:ls

The window function $w(\mathbf{x}_0)$ for a focused source can be calculated as

`secondary_source_selection.m`

$$
w(\mathbf{x}_0) = \begin{cases} 1 & \mathbf{n}_\mathrm{s}(\mathbf{x}_\mathrm{s}-\mathbf{x}_0)>0 \\ 0 & \text{else} \end{cases}
$$

(84)

#wfs:fs:selection

2.5.3 *Local Sound Field Synthesis*

The reproduction accuracy of WFS is limited due to practical aspects. For the audible frequency range the desired sound field can not be synthesized aliasing-free over an extended listening area, which is surrounded by a discrete ensemble of individually driven loudspeakers. However, it is suitable for certain applications to increase reproduction accuracy inside a smaller (local) listening region while stronger artifacts outside are permitted. The implemented Local Wave Field Synthesis method utilizes focused sources as a distribution of virtual loudspeakers which are placed more densely around the local listening area. These virtual loudspeakers can be driven by conventional SFS techniques, like e.g. WFS or NFC-HOA. The results are similar to band-limited NFC-HOA, with the difference that the form and position of the enhanced area can freely be chosen within the listening area.

The set of focused sources is treated as a virtual loudspeaker distribution and their positions $\mathbf{x}_{\mathrm{fs}}$ are subsumed under $\mathcal{X}_{\mathrm{fs}}$. Therefore, each focused source is driven individually by $D_l(\mathbf{x}_{\mathrm{fs}}, \omega)$, which in principle can be any driving function for real loudspeakers mentioned in previous sections. At the moment however, only WFS and NFC-HOA driving functions are supported. The resulting driving function for a loudspeaker located at $\mathbf{x}_0$ reads

`driving_function_mono_localwfs.m`
`driving_function_mono_wfs_vss.m`

$$D(\mathbf{x}_0, \omega) = \sum_{\mathbf{x}_{\mathrm{fs}} \in \mathcal{X}_{\mathrm{fs}}} D_l(\mathbf{x}_{\mathrm{fs}}, \omega) D_{\mathrm{fs}}(\mathbf{x}_0, \mathbf{x}_{\mathrm{fs}}, \omega) \,, \tag{85}$$

#D:localwfs

which is superposition of the driving function $D_l\mathrm{fs}(\mathbf{x}_0, \mathbf{x}_{\mathrm{fs}}, \omega)$ reproducing a single focused source at $\mathbf{x}_{\mathrm{fs}}$ weighted by $D_l(\mathbf{x}_{\mathrm{fs}}, \omega)$. Former is derived by replacing $\mathbf{x}_{\mathrm{s}}$ with $\mathbf{x}_{\mathrm{fs}}$ in the WFS driving functions (79) and (82) for focused sources. This yields

$$D_{\mathrm{fs}}(\mathbf{x}_0, \mathbf{x}_{\mathrm{fs}}, \omega) = \frac{1}{2\pi} A(\omega) w(\mathbf{x}_0) \mathrm{i} \frac{\omega}{c} \frac{(\mathbf{x}_0 - \mathbf{x}_{\mathrm{fs}}) \mathbf{n}_{\mathbf{x}_0}}{|\mathbf{x}_0 - \mathbf{x}_{\mathrm{fs}}|^{3/2}} \mathrm{e}^{\mathrm{i}\frac{\omega}{c}|\mathbf{x}_0 - \mathbf{x}_{\mathrm{fs}}|} \tag{86}$$

and

$$D_{\mathrm{fs},2.5\mathrm{D}}(\mathbf{x}_0, \mathbf{x}_{\mathrm{fs}}, \omega) = \frac{g_0}{2\pi} A(\omega) w(\mathbf{x}_0) \sqrt{\mathrm{i} \frac{\omega}{c}} \frac{(\mathbf{x}_0 - \mathbf{x}_{\mathrm{s}}) \mathbf{n}_{\mathbf{x}_0}}{|\mathbf{x}_0 - \mathbf{x}_{\mathrm{s}}|^{3/2}} \mathrm{e}^{\mathrm{i}\frac{\omega}{c}|\mathbf{x}_0 - \mathbf{x}_{\mathrm{s}}|} \,. \tag{87}$$

for the 2.5D case. For the temporal domain, inverse Fourier transform yields the driving signals

`driving_function_imp_localwfs.m`
`driving_function_imp_wfs_vss.m`

$$d(\mathbf{x}_0, t) = \sum_{\mathbf{x}_{\mathrm{fs}} \in \mathcal{X}_{\mathrm{fs}}} d_l(\mathbf{x}_{\mathrm{fs}}, t) * d_{\mathrm{fs}}(\mathbf{x}_0, \mathbf{x}_{\mathrm{fs}}, t) \,, \tag{88}$$

#d:localwfs

while $d_{\mathrm{fs}}(\mathbf{x}_0, \mathbf{x}_{\mathrm{fs}}, t)$ is derived analogously to (85) from (81) or (82). At the moment $d_l(\mathbf{x}_{\mathrm{fs}}, t)$ does only support driving functions from WFS.

Formula reference mapping

Bibliography

Abramowitz, M. and I. A. Stegun. *Handbook of Mathematical Functions*. Washington: National Bureau of Standards, 1972.

Ahrens, J. *Analytic Methods of Sound Field Synthesis*. New York: Springer, 2012.

Ahrens, J. and S. Spors. "On the Secondary Source Type Mismatch in Wave Field Synthesis Employing Circular Distributions of Loudspeakers". In: *127th Audio Engineering Society Convention*. 2009, Paper 7952.

– "Sound Field Reproduction Using Planar and Linear Arrays of Loudspeakers". *IEEE Transactions on Audio, Speech, and Language Processing* 18.8 (2010), pp. 2038–50.

– "Spatial encoding and decoding of focused virtual sound sources". In: *International Symposium on Ambisonics and Spherical Acoustics*. 2009.

Arfken, G. B. and H. J. Weber. *Mathematical Methods for Physicists*. Amsterdam: Elsevier, 2005.

Avni, A. et al. "Spatial perception of sound fields recorded by spherical microphone arrays with varying spatial resolution". *The Journal of the Acoustical Society of America* 133.5 (2013), pp. 2711–21.

Berkhout, A. "A holographic approach to acoustic control". *Journal of the Audio Engineering Society* 36.12 (1988), pp. 977–95.

Blauert, J. *Spatial Hearing*. The MIT Press, 1997.

Blumlein, A. D. "Improvements in and relating to Sound-transmission, Sound-recording and Sound-reproducing Systems". *Journal of the Audio Engineering Society* 6.2 (1958), pp. 91–98, 130.

Bracewell, R. N. *The Fourier Transform and its Applications*. Boston: McGraw Hill, 2000.

Colton, D. and R. Kress. *Integral Equation Methods in Scattering Theory*. New York: Wiley, 1983.

Donoho, D. L. et al. "Reproducible Research in Computational Harmonic Analysis". *Computing in Science & Engineering* 11.1 (2009), pp. 8–18.

Fazi, F. M. "Sound Field Reproduction". PhD thesis. University of Southampton, 2010.

Fazi, F. M. and P. A. Nelson. "Sound field reproduction as an equivalent acoustical scattering problem". *The Journal of the Acoustical Society of America* 134.5 (2013), pp. 3721–9.

Frank, M. "Phantom Sources using Multiple Loudspeakers". PhD thesis. University of Music and Performing Arts Graz, 2013.

Gerzon, M. A. "Periphony: With-Height Sound Reproduction". *Journal of the Audio Engineering Society* 21.1 (1973), pp. 2–10.

Gumerov, N. A. and R. Duraiswami. *Fast Multipole Methods for the Helmholtz Equation in Three Dimensions*. Amsterdam: Elsevier, 2004.

Hamasaki, K., K. Hiyama, and H. Okumura. "The 22.2 Multichannel Sound System and Its Application". In: *118th Audio Engineering Society Convention*. 2005, Paper 6406.

Herrin, D. W. et al. "A New Look at the High Frequency Boundary Element and Rayleigh Integral Approximations". In: *Noise & Vibration Conference and Exhibition*. 2003.

Ince, D. C., L. Hatton, and J. Graham-Cumming. "The case for open computer programs". *Nature* 482.7386 (2012), pp. 485–88.

Lax, M. and H. Feshbach. "On the Radiation Problem at High Frequencies". *The Journal of the Acoustical Society of America* 19.4 (1947), pp. 682–90.

Leakey, D. M. "Some Measurements on the Effects of Interchannel Intensity and Time Differences in Two Channel Sound Systems". *The Journal of the Acoustical Society of America* 31.7 (1959), pp. 977–86.

Moncel, T. du. "The international exhibition and congress of electricity at Paris". *Nature* October 20 (1881), pp. 585–89.

Morse, P. M. and H. Feshbach. *Methods of Theoretical Physics*. Minneapolis: Feshbach Publishing, 1981.

Pulkki, V. "Virtual Sound Source Positioning Using Vector Base Amplitude Panning". *Journal of the Audio Engineering Society* 45.6 (1997), pp. 456–66.

Schultz, F. and S. Spors. "Comparing Approaches to the Spherical and Planar Single Layer Potentials for Interior Sound Field Synthesis". *Acta Acustica* 100.5 (2014), pp. 900–11.

Spors, S. and J. Ahrens. "Reproduction of Focused Sources by the Spectral Division Method". In: *International Symposium on Communications, Control and Signal Processing*. 2010.

Spors, S., V. Kuscher, and J. Ahrens. "Efficient realization of model-based rendering for 2.5-dimensional near-field compensated higher order Ambisonics". In: *IEEE Workshop on Applications of Signal Processing to Audio and Acoustics*. 2011, pp. 61–64.

Spors, S., R. Rabenstein, and J. Ahrens. "The Theory of Wave Field Synthesis Revisited". In: *124th Audio Engineering Society Convention*. 2008, Paper 7358.

Spors, S. and F. Zotter. "Spatial Sound Synthesis with Loudspeakers". In: *Cutting Edge in Spatial Audio, EAA Winter School*. 2013, pp. 32–37.

Start, E. W. "Direct Sound Enhancement by Wave Field Synthesis". PhD thesis. Technische Universiteit Delft, 1997.

Steinberg, J. and W. B. Snow. "Symposium on wire transmission of symphonic music and its reproduction in auditory perspective: Physical Factors". *Bell System Technical Journal* 13.2 (1934), pp. 245–58.

Verheijen, E. "Sound Reproduction by Wave Field Synthesis". PhD thesis. Technische Universiteit Delft, 1997.

Wierstorf, H. "Perceptual Assessment of Sound Field Synthesis". PhD thesis. Technische Universität Berlin, 2014.

Wierstorf, H., A. Raake, and S. Spors. "Binaural assessment of multi-channel reproduction". In: *The technology of binaural listening*. Ed. by J. Blauert. New York: Springer, 2013, pp. 255–78.

Wierstorf, H. and S. Spors. "Sound Field Synthesis Toolbox". In: *132nd Audio Engineering Society Convention*. 2012, eBrief 50.

Williams, E. G. *Fourier Acoustics*. San Diego: Academic Press, 1999.

Yon, S., M. Tanter, and M. Fink. "Sound focusing in rooms: The time-reversal approach". *The Journal of the Acoustical Society of America* 113.3 (2003), pp. 1533–43.

Zotter, F. and S. Spors. "Is sound field control determined at all frequencies? How is it related to numerical acoustics?" In: *52nd Audio Engineering Society Conference*. 2013, Paper 1.3.